

Frequency Reconfigurable Fractal CPW-Fed Antennas Designed for Telecommunication Applications

Sondos Mehri¹, Ines Rouissi¹, Hatem Rmili¹, Bandar Hakim¹, and Raj Mittra^{1,2}

¹Electrical and Computer Engineering Department, Faculty of Engineering
King Abdulaziz University, P.O. Box 80204, Jeddah 21589, Saudi Arabia
hmrili@kau.edu.sa

²Electrical and Computer Engineering Department
University of Central Florida, EMC Lab, Orlando, FL 32816, USA
rajmittra@ieee.org

Abstract — A frequency reconfigurable fractal antenna for wireless communication application is presented in this paper. Three RF switches are incorporated into the antenna design to achieve frequency reconfigurability. The proposed antenna is designed and simulated using the HFSS code and then fabricated. The experimental results confirm the numerical simulation and demonstrate that integrating the RF switches improves the antenna flexibility and enables us to switch the antenna from single-band to dual-band as well as to a multi-band state with minimal design complexity and high degree of miniaturization.

Index Terms — Frequency reconfigurability, notched band, ultrawide band, varactor diode.

I. INTRODUCTION

Recent rapid growth in wireless and communication technologies has prompted us to create new and more advanced antennas capable of operating in multiple bands. Wireless standards such as GSM 800/900 and GSM 1800/1900 govern the operation in the lower UHF band, while WIFI and WIMAX do the same in the upper UHF band. Recently, frequency reconfigurable antennas have been proposed to achieve multiband operation [1-5], as opposed to fixed antennas which can only operate in a frequency band. Reconfigurable antennas are capable of dynamically altering their performance in order to adapt to environmental conditions and to meet system requirements that can be complex, and for this purpose various reconfiguration techniques have been investigated [6, 7]. Approaches based on electrical switching circuits, such as RF-switches and varactors [8-11] represent the most commonly used tuning techniques owing to the simplicity of their integration into the antenna system and their

capability of rapid switching. These switching elements are often used at specific locations in an antenna to modify its current distribution and, thereby modify its RF properties. Despite providing multiband operation, the antenna maintains its compactness and light weight feature to facilitate its integration with other microwave components in a device. Toward this goal, the fractal technique is adopted in this work to improve the size of the antenna in comparison to non-fractal design [12-14]. Such a design has the salutary features of low profile, multi-frequency operation, impedance compatibility and ease of integration for different wireless application systems.

In this paper we propose a frequency reconfigurable Hilbert curve CPW-fed antenna which is, designed and fabricated. This work is inspired by the antenna designs presented in our previous work [15], but with enhanced performance achieved by incorporating RF switches to realize frequency reconfigurable characteristics. Three RF switches are placed across the arms of the antenna and enable the antenna to operate in multiple bands by altering the switches states. To validate the simulation results, the Hilbert curve reconfigurable antenna is fabricated, and tested. The measurement results confirm that the proposed antenna is capable of operating in three different states, namely single-band, dual-band and multi-band for a small area of dimensions of $17 \times 23 \text{ mm}^2$. So, the main merit of the proposed design lies in achieving, multiband switching operations, acceptable gain with minimal complexity and high degree of miniaturization.

The remainder of the paper is organized as follows. The next section describes the antenna structure and fractal design. Simulation and experimental results are presented and discussed in Section 3. Finally, the last section presents the conclusions of this study.

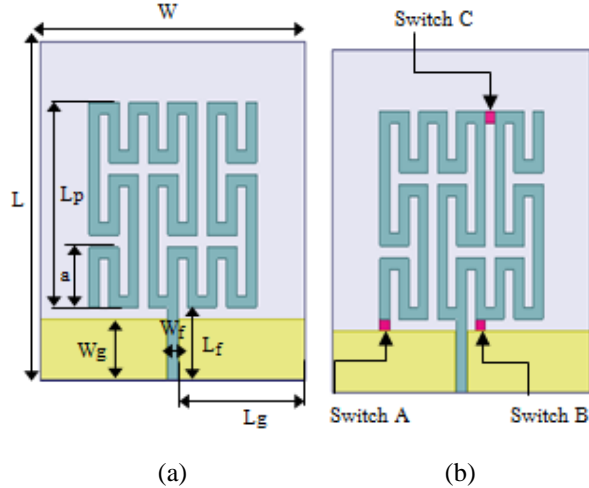


Fig. 1. Geometry of the planar fractal CPW-fed antenna: (a) reference structure, and (b) incorporation of three switches: A, B, and C.

Table 1: Geometric parameters of the proposed design

Parameters	Dimensions (mm)
Substrate width	27
Substrate length	28
Antenna length	17
Metal width	1
Hilbert curve length at the second iteration	5
Substrate width	1
Microstrip feed width	6
Microstrip feed length	5
Ground width	12.89
Ground length	1
Ground and Microstrip feed spacing	1

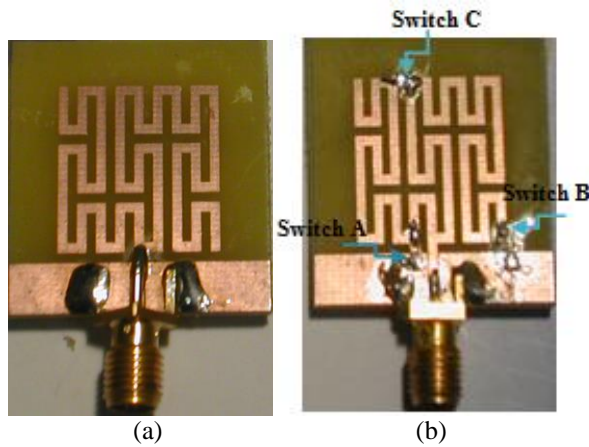


Fig. 2. Prototypes of the fabricated antennas: (a) reference structure, and (b) antenna prototype with the integration of A, B, and C switches.

Table 2: Switch configuration of the antenna design

States	Switches		
	A	B	C
1	OFF	OFF	OFF
2	OFF	OFF	ON
3	OFF	ON	OFF
4	OFF	ON	ON
5	ON	OFF	OFF
6	ON	OFF	ON
7	ON	ON	OFF
8	ON	ON	ON

II. ANTENNA DESIGN

The geometry of the reference antenna design is presented in Fig. 1 (a). This figure shows the compact fractal antenna presented in our previous work [15]. The design uses the second iteration of the Hilbert curve, whose geometrical parameters are provided in Table 1. To reconfigure the reference structure in specific bands, we propose a new design which uses RF switches, inserted in specific locations as shown in Fig. 1 (b). The inserted switches are denoted A, B, and C where, A and B are placed between the ground and the antenna while C is located on the upper arms of the antenna. The proposed structures are printed on FR4 substrate of thickness 0.8 mm, relative dielectric constant $\epsilon_r = 4.4$ and loss tangent $\delta = 0.02$. Figure 2 shows the prototypes of the fabricated antennas in which three RF switches have been integrated. The switch itself has two states these are: State 1, when the switch is OFF and State 2, when the switch is ON. As indicated in Table 2, eight possible switching states are provided by the three incorporated switches.

III. RESULTS AND DISCUSSIONS

A. Reflection coefficient S_{11}

The variation of the input reflection coefficient vs. the frequency is shown in Fig. 3 for each state. In this figure simulated S_{11} curves corresponding to the eight operating states are compared to the measured S_{11} . Inspection of these figures shows that there is good agreement between the measured and simulated results. The measured results show that, the proposed antenna can be made to resonate at eight different frequencies by using various combinations of the switches A, B, and C. The experimental results for different states are summarized in Table 3, which shows that the proposed antenna generates fifteen frequencies in the frequency range of 0.8 GHz to 4.7 GHz. As shown in this table, State 1 resonates at four frequencies, State 2 at three frequencies, while State 5 and state 7 resonate at two other frequencies. For all other states, one resonance is realized per state. Experimental results show also that the proposed antenna is able to cover various bands. As and (h) State 8. An example, the antenna covers 4 bands

when operating in state 1 and three bands for State 2; hence a dual-band operation is obtained for both states 5 and 7. However, a single band per state is obtained for the remaining states. These results demonstrate the fact that the ability of the proposed antenna to achieve frequency agility which, in turn, makes it suitable for use in wireless communication systems. It is worth to note that an acceptable agreement between numerical and experimental results is obtained expect for some specific states (notably when switches A and B are

activated). This small disagreement reported for states 3 and 5 is due to the fact that switches A and B are connected to the antenna ground plane which influences the antenna behavior. In fact, the surface currents flowing on the ground plane may affect the switches, and then the input reflection coefficient of the antenna. In addition, the coaxial connector effect was not taken into consideration in our simulated model, which may explain also the difference between simulation and measurements [8].

Table 3: Performances summary of the proposed antenna for different states

States	Number of Resonated Frequency		Operating Bands (GHz)	
	Simulation	Measurement	Simulation	Measurement
1	4	4	0.8-10; 1.2-1.4; 2.2-3.8	0.9-1.0; 1.4-1.5; 2.7-3.2; 3.5-3.8
2	3	3	0.8-1.1; 1.9-3.2; 3.7-4.2	2.5-3.14; 3.7-3.9; 4.7
3	2	1	1.2-1.3; 4.4-4.7	4.45-4.71
4	1	1	4.1-4.4	3.8-4.3
5	1	2	3.6-3.8	0.95-1; 4.5-4.6
6	1	1	3.7-4.0	4.5-4.7
7	2	2	2.6; 4.5	2.6; 4.5
8	1	1	2.4-2.6	2.4-2.6

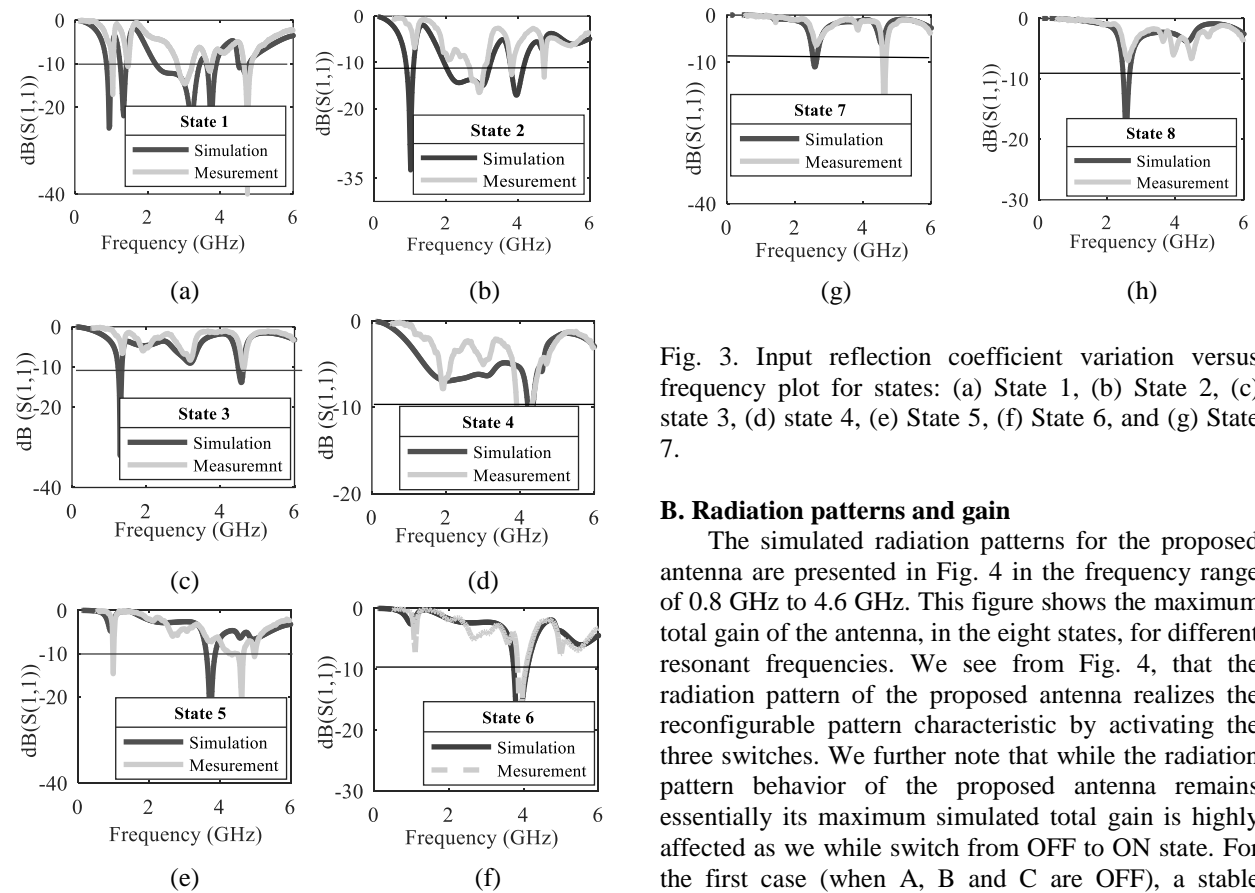


Fig. 3. Input reflection coefficient variation versus frequency plot for states: (a) State 1, (b) State 2, (c) state 3, (d) state 4, (e) State 5, (f) State 6, and (g) State 7.

B. Radiation patterns and gain

The simulated radiation patterns for the proposed antenna are presented in Fig. 4 in the frequency range of 0.8 GHz to 4.6 GHz. This figure shows the maximum total gain of the antenna, in the eight states, for different resonant frequencies. We see from Fig. 4, that the radiation pattern of the proposed antenna realizes the reconfigurable pattern characteristic by activating the three switches. We further note that while the radiation pattern behavior of the proposed antenna remains essentially its maximum simulated total gain is highly affected as we while switch from OFF to ON state. For the first case (when A, B and C are OFF), a stable

radiation pattern is observed. An omni-directional radiation pattern in the (yoz) plane is shown with a maximum total gain of -2.2 dB at $f = 3.74$ GHz. For the second case per state (State 2, State 3, and State 5), the radiation pattern retains the same omni-directional behavior when one switch is activated, and its maximum total gain is 0.4 dB at 3.84 GHz. For the third case, when two switches are activated per state (State 6 and State 7), the radiation pattern is still omni-directional, and has a maximum total gain of -3.8 dB for $f = 3.84$ dB. Similar characteristics are also obtained for the last case, when all the switches are activated (State 8). Measured radiation pattern obtained by activating the A, B, and C switches states are presented in Fig. 5 to validate the simulation results. This figure shows that the measured gain varies from -11.54 dB to -2 dB in the lower band (0.9-2.11 GHz), and from -2.4 dB to 5 dB in the upper band (3-4.7 GHz). The results of maximum measured gain the different states are summarized in Table 4. The table, which compares the gain performances of the proposed antenna for different switches states, shows

that the gain of the antennas is highly affected when the switch B is activated. Table 4 also measurements shows that, the lower measured gain is adversely affected when the switches A and B are activated (corresponding states are: 3, 4, 5, 6, 7, and 8). As explained earlier, this degradation is caused by the coupling between the ground plane and the switches.

Table 4: Maximum measured gain for different states

States	Frequency (GHz)	Maximum Measured Gain (dB)
1	4.7	3.02
2	3.8	5
3	4.6	0.3
4	4.63	0.31
5	4.6	1.9
6	3.9	4.7
7	4.6	0.31
8	2.6	-0.13

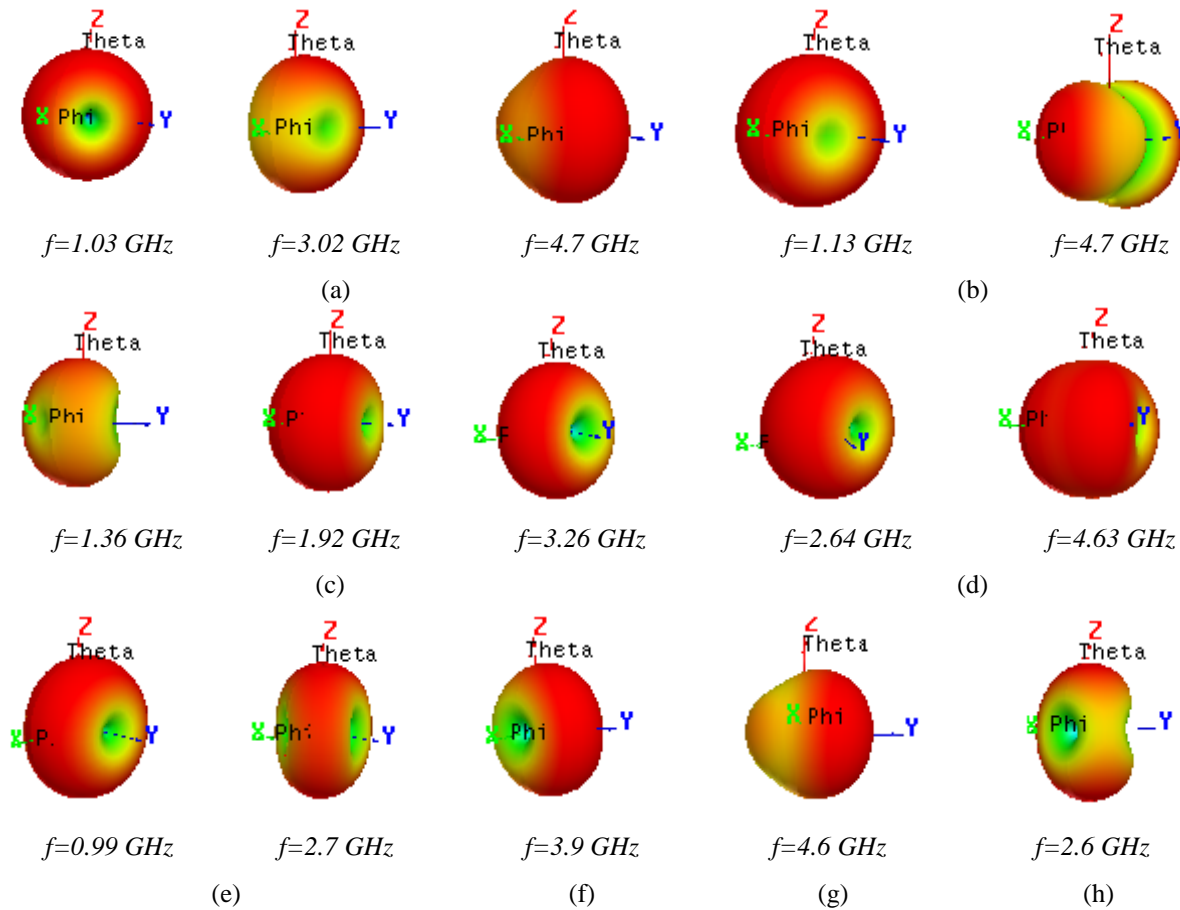


Fig. 4. 3D simulated radiation patterns for states: (a) State 1, (b) State 2, (c) State 3, (d) State 4, (e) State 5, (f) State 6, (g) State 7, and (h) State 8.

C. Comparative study

To mark the advantages of the proposed design compared to those reported in literature, a comparative study was performed, and results are summarized in Table 5. We can note from Table 5 that better performances in terms of size, design complexity are achieved with the proposed design. For example, the design proposed in [16] giving higher gain and more

operating bands is achieved at the expense of the antenna size and the design complexity. In fact, by referring to Table 5, the antenna size is 4 times larger than our proposed design, and the number of PIN diodes is 8 instead of 3. So, our structure succeeds in achieving high degree of miniaturization, multiband switching capabilities with acceptable gain and minimum number of PIN diodes.

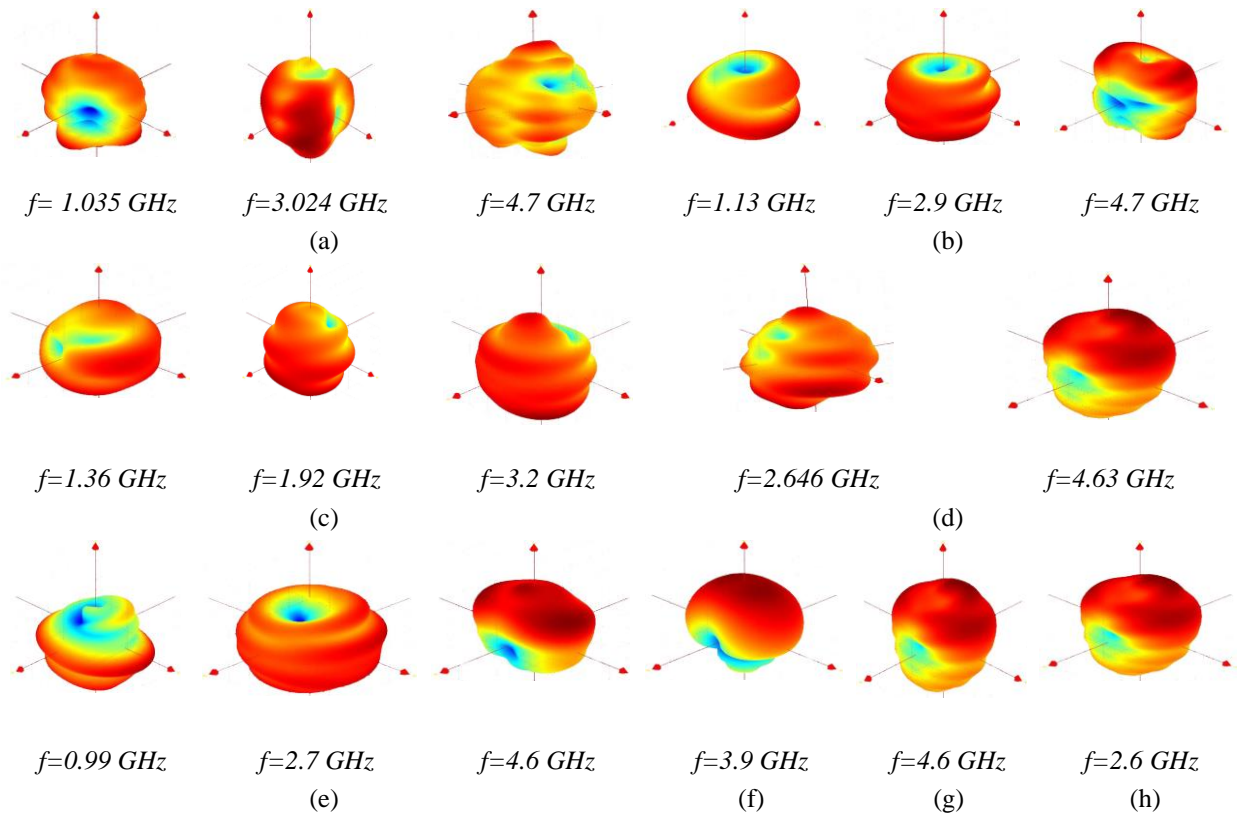


Fig.5. 3D measured radiation patterns for states: (a) State 1, (b) State 2, (c) State 3, (d) State 4, (e) State 5, (f) State 6, (g) State 7, and (h) State 8.

Table 5: Comparison of the proposed fractal multiband antenna (e) with those present in the state-of-art literature

Ref.	Antenna Design Geometry	Number of PIN Diodes	Max. Gain (dB)	Total Area (mm ²)	Number of Operating Bands
[17]	No Fractal	4	2.5	58.8 × 40	3
[18]	No Fractal	5	3.2	25 × 45	5
[19]	Fractal	6	-11.37	30 × 30	13
[16]	Fractal	8	6.8	80 × 80	18
[20]	Fractal	1	5.36	35 × 30	5
[21]	Fractal	2	4	35 × 30	6
Prop.	Fractal	3	4.7	17 × 23	14

IV. CONCLUSION

A frequency reconfigurable antenna has been designed, analyzed and fabricated in this paper. To achieve reconfigurability characteristics, three switches

were incorporated in the designed antennas which were fabricated and experimentally evaluated to validate the simulated results. The designed reconfigurable antenna, which can operate in one, two, three and four bands,

has a total area of $17 \times 23 \text{ mm}^2$. So, the proposed design success in achieving, multiband switching operations, acceptable gain with minimal complexity and high degree of miniaturization. Such features provided by the proposed antenna makes it suitable for use in telecommunication devices that operate in multiple frequency bands.

ACKNOWLEDGMENT

This project was funded by the Deanship of Scientific Research (DSR), King Abdulaziz University, under Grant No. KEP-Msc-3-135-39. The authors, therefore, acknowledge technical and financial support of KAU.

The authors are grateful to the help of Dr Jean-Marie Floch from the IETR institute, INSA Rennes, France, for his helps during experiments.

REFERENCES

- [1] Z. Hao and J. Hu, "Design of a frequency and polarization reconfigurable patch antenna with a stable gain," *IEEE Access*, vol. 6, pp. 68169-68175, 2018.
- [2] M. A. Alam and A. Abbosh, "Reconfigurable band-rejection antenna for ultra-wideband applications," *IET Microwaves, Antennas & Propagation*, vol. 12, no. 2, pp. 195-202, 2018.
- [3] S. K. Beheraa and Y. K. Choukiker, "Wideband frequency reconfigurable Koch snowflake fractal antenna," *IET Microwaves, Antennas & Propagation*, vol. 11, no. 2, pp. 203-208, 2017.
- [4] I. Rouissi, J. M. Floch, H. Rmili, and H. Trabelsi, "Design of a frequency reconfigurable patch antenna using capacitive loading and varactor diode," *European Conference on Antennas and Propagation*, 2015.
- [5] I. B. Trad, J. M. Floch, H. Rmili, L. Laadhar, and M. Drissi, "Planar elliptic broadband antenna with wide range reconfigurable narrow notched bands for multi-standard wireless communication devices," *Progress in Electromagnetic Research*, vol. 146, pp. 69-80, 2014.
- [6] V. Arun, L. R. Karlmarx, K. J. J. Kumar, and C. Vimlitha, "N-shaped frequency reconfigurable antenna with auto switching unit," *ACES Journal*, vol. 33, no. 6, pp. 710-713, 2018.
- [7] S. Chilukuri, K. Dahal, A. Lokam, and W. Chen, "A CPW fed T-shaped frequency reconfigurable antenna for multi radio applications," *ACES Journal*, vol. 33, no. 11, pp. 1276-1285, 2018.
- [8] B. Babakhani, S. K. Sharma, and N. R. Labadie, "A frequency agile microstrip patch phased array antenna with polarization reconfiguration," *IEEE Transactions on Antennas and Propagation*, vol. 64, no. 10, pp. 4316-4327, 2016.
- [9] R. Herzi, M. Bouslama, L. Osman, and A. Gharsallah, "Frequency agile Vivaldi antenna with enhanced gain for wireless applications," *IEEE MTT-S International Microwave Workshop Series on Advanced Materials and Processes for RF and THz Applications*, 2017.
- [10] I. B. Trad, H. Rmili, J. M. Floch, and H. Zangar, "Design of planar mono-band rejected UWB CPW-Fed antennas for wireless communications," *Mediterranean Microwave Symposium*, 2011.
- [11] S. Dakhli, H. Rmili, J. M. Floch, M. Sheikh, K. Mahdjoubi, F. Choubani, and R. Ziolkowski, "Capacitively loaded loop-based antennas with reconfigurable radiation patterns," *International Journal on Antennas and Propagation*, pp. 1-10, 2015.
- [12] J. Zhou, X. Wu, B. You, Y. P. Shang, J. Huang, and T. Huang, "A band-notched UWB antenna loaded with tree-shaped fractal," *Progress in Electromagnetics Research Symposium*, 2018.
- [13] R. M. H. Bilal, A. A. Rahim, H. Maab, and M. M. Ali, "Modified wang shaped ultra-wideband (UWB) fractal patch antenna for millimetre-wave applications," *Progress in Electromagnetics Research Symposium*, 2018.
- [14] S. Srivastava, P. Mishra, and R. K. Singh, "Design of a reconfigurable antenna with fractal geometry," *IEEE UP Section Conference on Electrical Computer and Electronics*, 2015.
- [15] I. Rouissi, I. B. Trad, J. M. Floch, M. Sheikh, and H. Rmili, "Design of miniature multiband fractal CPW-fed antenna for telecommunication applications," *Progress in Electromagnetics Research Symposium*, 2013.
- [16] H. Altun, E. Korkmaz, and B. Türetken, "Reconfigurable fractal tree antenna for multiband applications," *URSI General Assembly and Scientific Symposium*, 2011.
- [17] S. Sharma and C. C. Tripathi, "Frequency reconfigurable U-slot antenna for SDR application," *Progress In Electromagnetics Research Letters*, vol. 55, pp. 129-136, 2015.
- [18] L. Pazin and Y. Leviatan, "Reconfigurable slot antenna for switchable multiband operation in a wide frequency range," *IEEE Antennas and Wireless Propagation Letters*, vol. 12, pp. 329-332, 2013.
- [19] Y. B. Chaouche, F. Bouttout, I. Messaoudene, L. Pichon, M. Belazzoug, and F. Chetouah, "Design of reconfigurable fractal antenna using pin diode switch for wireless applications," *Mediterranean Microwave Symposium*, 2016.
- [20] T. Alia, N. Fatimab, and R. C. Biradar, "A miniaturized multiband reconfigurable fractal slot antenna for GPS/GNSS/Bluetooth/WiMAX/X-band

applications,” *International Journal of Electronics and Communications*, vol. 94, pp. 234-243, 2018.

- [21] P. Pokkunuri, B. T. P. Madhav, G. K. Sai, M. Venkateswararao, B. Ganesh, N. Tarakaram, and D. P. Teja, “Metamaterial inspired reconfigurable fractal monopole antenna for multiband applications,” *International Journal of Intelligent Engineering and Systems*, vol. 12, no. 2, pp. 53-61, 2019.



Sondos Mehri has received the Ph.D. degree in 2017 in Electrical Engineering, from the National School of Engineering in Tunis (ENIT), Tunisia and is currently working as a Postdoctoral Researcher under the supervision of Prof. Raj Mittra. Her research interests are focused on the design of a substrate integrated waveguide slot array for millimeter waves frequencies.

Mehri has been awarded the 2nd Prize of Students Paper Poster Competition of the IEEE Melecon in 2016.



Hatem Rmili received the B.S. degree in General Physics from the Science Faculty of Monastir, Tunisia in 1995, and the DEA diploma from the Science Faculty of Tunis, Tunisia, in Quantum Mechanics, in 1999. He received the Ph.D. degree in Physics (Electronics) from both the University of Tunis, Tunisia, and the University of Bordeaux 1, France, in 2004. From December 2004 to March 2005, he was a Research Assistant in the PIOM Laboratory at the University of Bordeaux 1. During March 2005 to March 2007, he was a Postdoctoral Fellow at the Rennes Institute of Electronics and Telecommunications, France. From March to September 2007, he was a Postdoctoral Fellow at the ESEO Engineering School, Angers, France. From September 2007 to August 2012, he was an Associate Professor with the Mahdia Institute of Applied Science and Technology (ISSAT), Department of Electronics and Telecommunications, Tunisia. Actually, he is Associate Professor with the Electrical and Computer Engineering Department, Faculty of Engineering, King Abdulaziz University, Jeddah, Saudi Arabia. His main research activities concern antennas, metamaterials and metasurfaces.



Bandar Hakim is an Assistant Professor of Electrophysics at KAU. He received his Ph.D. degree in Electrophysics from the University of Maryland. He worked with the Medical Robotics group at the École Polytechnique Fédérale de Lausanne in Switzerland, the Center for Devices and Radiological Health at the Food and Drug Administration in Washington DC and the Neurology Department at Mount Sinai School of Medicine in the New York NY. He served as an Industrial Consultant in the US, Switzerland and Germany.



Raj Mittra is a Professor in the Department of Electrical & Computer Science of the University of Central Florida in Orlando, FL., where he is the Director of the Electromagnetic Communication Laboratory. Prior to joining the University of Central Florida, he worked at Penn State as a Professor in the Electrical and Computer Engineering from 1996 through June 2015. He also worked as a Professor in the Electrical and Computer Engineering at the University of Illinois in Urbana Champaign from 1957 through 1996, when he moved to the Penn State University. Currently, he also holds the position of Hi-Ci Professor at King Abdulaziz University in Saudi Arabia.

He is a Life Fellow of the IEEE, a Past-President of AP-S, and he has served as the Editor of the Transactions of the Antennas and Propagation Society. He won the Guggenheim Fellowship Award in 1965, the IEEE Centennial Medal in 1984, and the IEEE Millennium medal in 2000. Other honors include the IEEE/AP-S Distinguished Achievement Award in 2002, the Chen-To Tai Education Award in 2004 and the IEEE Electromagnetics Award in 2006, and the IEEE James H. Mulligan Award in 2011.

Mittra is a Principal Scientist and President of RM Associates, a consulting company founded in 1980, which provides services to industrial and governmental organizations, both in the U.S. and abroad.